

Novel Benzimidazole Analogs as Inhibitors of EGFR Tyrosine Kinase

Soni Yadav^{1,2}, Deepa Sinha³, Sanjay K. Singh² and Vinay K. Singh^{1,*}

¹Department of Chemistry, DrKNMIET, Modinagar, Meerut 201204, India

²Department of Applied Sciences, Institute of Engineering and Technology, Lucknow 226021, India

³Department of Applied Sciences, HMRITM (Affiliated to GGSIP University), Delhi 110036, India

*Corresponding author: V. K. Singh, vinayk2003@rediffmail.com

A series of new benzimidazole congeners were synthesized, and their structures were elucidated on the basis of elemental analyses and spectral studies (¹H NMR, FT-IR and EI-MS). Preliminary pharmacokinetic studies showed a promising outlook for further *in vivo* evaluation. The newly synthesized compounds were tested *in vitro* on human breast carcinoma cell line (MCF-7) in which EGFR is highly expressed. Most of the tested compounds exhibited antitumor activity with IC₅₀ values in the micro to nano molar range.

Key words: antitumor, benzimidazole, EGFR, nanomolar, spectroscopy

Received 13 February 2012, revised 19 March 2012 and accepted for publication 9 April 2012

Benzimidazoles and related derivatives are a class of fused heterocycles that are of considerable interest because of the diverse range of their biological properties, for example, anticancer, diuretic, anti-inflammatory, anticonvulsant, and antihypertensive activities (1–9). They also demonstrate several other useful and interesting properties such as hypertensive adrenergic blocker, selective phosphodiesterase inhibitor, against prostate disorders, and dihydrofoalate reductase inhibitor (10–18).

In addition, some derivatives are calcium antagonists and share the common property of interfering with the influx of extracellular calcium via the calcium L channel. Recently, quinoxaline chemistry has found new direction because of some resemblance with folic acid (19,20).

Protein tyrosine kinases are enzymes involved in many cellular processes such as cell proliferation, metabolism, survival, and apoptosis. Several protein tyrosine kinases are known to be activated in cancer cells and to drive tumor growth and progression. Blocking tyrosine kinase activity therefore represents a rational approach to

cancer therapy. Protein kinases (PTKs) catalyze the phosphorylation of tyrosine and serine/threonine residues in various proteins involved in the regulation of all functions (21). They can be broadly classified as receptor such as epidermal growth factor receptor (EGFR), or non-receptor kinases. Inappropriate or uncontrolled activation of many of these kinases, by over-expression, constitutive activation, or mutation, has been shown to result in uncontrolled cell growth (22). The epidermal growth factor receptor belongs to the family of transmembrane growth factor receptor PTKs. The EGFR erbB1 and erbB2 PTKs have been identified as interesting targets for medicinal chemistry programs especially in cancer therapy. Excellent descriptions of the involvement of erbB family proteins in cell physiology and disease applications have been reported and reviewed (23–26).

Overexpression of these receptors was found in a number of cancers (e.g., breast, ovarian, colon, and prostate); their expression levels often correlate with vascularity and are associated with poor prognosis in patients (27). Inhibitors of the EGFR PTK are therefore expected to have great therapeutic potential in the treatment of malignant and non-malignant epithelial diseases. Drug discovery efforts have targeted this aberrant kinase activity in cancer, asthma, psoriasis, and inflammation (28). Recent advances in the identification of erbB family kinase inhibitors have created hope for the modulation of uncontrolled cell growth in cancer therapy for solid tumors (29). This strongly suggests that these targets represent drug intervention opportunities because of pivotal role in governing cellular proliferation, survival, and metastasis. A great number of different structural classes of tyrosine kinase inhibitors has been reported and reviewed (23–25). Recent success in the clinical evaluation of EGFR tyrosine kinase (TK) inhibitors such as gefitinib and erlotinib strongly suggests small molecular EGFR-TK inhibitors to be promising new anticancer drugs. The most promising small molecule selective EGFR-TK inhibitors include pyrrolopyrimidines, aminoquinazolines, and benzimidazole analogs.

In the same direction, and in continuing effort to find more potent selective lead compound, herein, we describe a series of benzimidazole conjugated with quinazoline derivatives mimicking gefitinib and erlotinib as possible antitumor agents that may act through EGFR inhibition.

Chemistry

The chemicals used in the synthesis are purchased from Aldrich and Merck and are of analytical grades. Analytical thin layer chro-

matography (TLC) on silica gel plates containing UV indicator was employed routinely to follow the course of reactions and to check the purity of products. All reagents and solvents were purified and dried by standard techniques. IR spectra were recorded on a PerkinElmer FT-IR series using KBr cell (PerkinElmer, Cambridge, MA, USA). NMR spectra were measured in CDCl_3 by Bruker 400 MHz apparatus with TMS as an internal standard. EI-MS spectra were recorded on a JEOL SX102/DA (KV 10 mA) instrument. Elemental analysis was performed on elemental analyzer Gmbh variable system. Radio complexation and radio chemical purity was checked by instant strip chromatography (silica gel impregnated paper chromatography) with ITLC-SG (Gellman Sciences, Ann Arbor, MI, USA). The gamma scintillation counting was carried out at ECA (Electronic Corporation of India Ltd., Hyderabad, India) Gamma Ray Spectrometer K 2700 B. All the reaction steps were monitored by TLC [chloroform:methanol:hexane 4:3:1].

QSAR analysis

The QSAR investigations were carried out by the linear-free energy relationship (LFER) model proposed by Hansch and Leo. The selection of parameters is the first step in any QSPR study. In this study, parameters that were considered relevant to the Schiff base series (electronic, hydrophobic, and steric) were selected and considered as consistent, which included molar refractivity, Vander Waals volume (VDW), Connolly accessible area, Connolly molecular area, Connolly solvent excluded area, dipole-dipole energy (DD), partition coefficient ($\log P$), HOMO, etc. The above-mentioned parameters were calculated by MM2 studies using Chem 3D 6.0 software (PerkinElmer Inc.). Geometries of all compounds were completely optimized by the same software package.

A classical Hansch multivariate regression analysis using the least-square method was chosen to derive QSAR equations for the data set. The level of significance of each coefficient was judged by statistical procedure such as F tests. Statistic analysis was carried out by employing the method of least square with stepwise selection and elimination procedure. For each equation, several indices of best fit were considered: the regression coefficient 'r', the standard deviation 's', and the measure of level of statistical significance 'F'.

Two models were found which are as follows:

QSAR Model for benzimidazole congeners (Model 1)

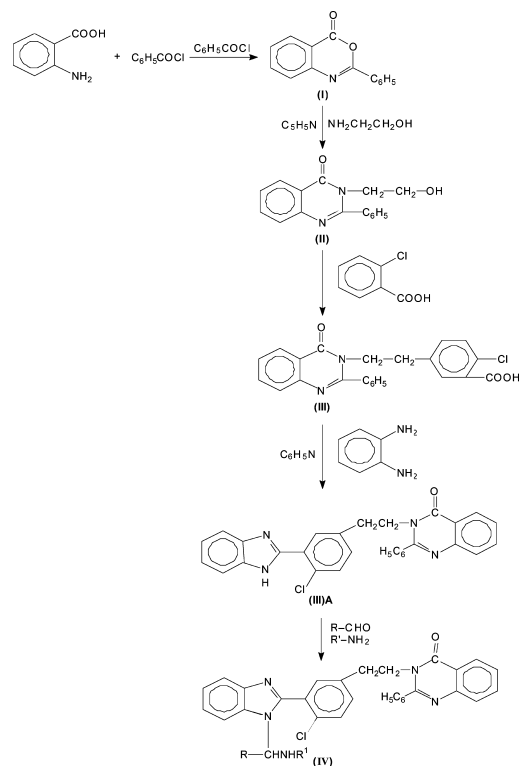
$$-\log C = 1.01432(\pm 0.5208) - \text{VDW } 0.0104(\pm 0.538)$$

$$n = 15 \quad |r| = 0.910 \quad s = 0.198 \quad F = 99.125$$

The synthetic steps were used as shown in Scheme 1.

Synthesis 2-Phenyl-3-[5-(2-chloro-3-carboxylatophenyl) ethyl] 4(3H)-quinazolone

A mixture of 2-phenyl-3-(hydroxy-ethyl) 4(3H) quinazolone (0.06 mol) and *o*-chloro benzoic acid (0.06 mol) was dissolved in concentrated sulfuric acid (50 mL) by stirring and cooling the reaction mixture occasionally. When a clear solution was obtained, the resultant solution was further stirred for 1 h at room temperature and was



Scheme 1: Chemical Scheme for synthesis of novel benzimidazoles.

left under refrigeration for 24 h. Subsequently, the acidified solution was poured into ice-cold water (100 mL) slowly and carefully with constant stirring. A solid that separated out was filtered off and washed with water repeatedly to remove any sulphonated products formed during the course of the reaction. The crude compound thus obtained was treated with an aqueous solution of sodium bicarbonate (10%). Evolution of carbon dioxide as effervescence was observed. A little more sodium bicarbonate solution was added to ensure the complete reaction with the carboxylic acid. When there was no more effervescence, the remaining solid was filtered off, and the filtrate was neutralized with diluted hydrochloric acid. The solid thus obtained was filtered off and washed with water. It was dried in vacuo and recrystallized from acetone as white crystalline needles, m.p. 148–149 °C [149 °C]¹³, yield, 70%.

2-Phenyl-3-[5-(2-(1H-benzimidazolyl)-2-chlorophenyl) ethyl] 4(3H) quinazolone

This step involves the cyclization of a carboxylic acid into a benzimidazole on reaction with *o*-phenylenediamine. Thus, 2-phenyl-3-[5-(2-chloro-3-carboxylatophenyl) ethyl] 4(3H) quinazolone and *o*-phenylenediamine in a molar ratio of (0.02 mol) and (0.025 mol), respectively, in dry pyridine (50 mL) were heated under reflux for 6 h under anhydrous reaction conditions. Subsequently, the contents after cooling to room temperature were poured into ice-cold diluted hydrochloric acid (100 mL). The solid that separated out was allowed to settle down and filtered off. It was washed successively with water and dried overnight under vacuum. Recrystallization from

diluted ethanol afforded 2-phenyl-3-[4-{2-(1H-benzimidazolyl)-2-chlorophenyl} 4(3H) quinazolone in analytically pure form. It melted at 184–185 °C, yield, 65%.

A mixture of 2-phenyl-3-[4-{2-(1H-benzimidazolyl) 2-chlorophenyl} ethyl] 4(3H) quinazolone (0.01 mol), an aromatic aldehyde (0.01 mol) and an aromatic primary amine (0.01 mol), was heated under reflux for 4 h under anhydrous reaction conditions. Subsequently, solvent ethanol was distilled off, and the remaining pasty mass was triturated with petroleum ether (b.p. 60–80 °C). It was treated with diluted hydrochloric acid (50 mL). Solidification occurred. The solid was filtered off and washed with 1% NaOH solution initially and finally with water. It was dried in vacuum and recrystallized from ethanol.

Radiolabeling of the compounds with Technetium

Radiolabeling of compounds was carried out by taking 100 μL of 0.03 nM solution of the compounds dissolved in DMSO and taken in a shielded vial. Further 60 μL of 1×10^{-2} M $\text{SnCl}_2 \cdot 2\text{H}_2\text{O}$ (dissolved in N_2 Purged 1 mL 10% acetic acid) was added followed by freshly eluted saline solution of sodium pertechnetate (NaTcO_4) (74 MBq, 100 mL). The pH of the reaction mixture was adjusted to 6.5 with 0.1 M NaHCO_3 solution and shaken to mix the contents well. The vial was allowed to incubate for 20–30 min at room temp. Labeling of the compound, radiochemical purity as well as R_f of the $^{99\text{m}}\text{Tc}$ -based complex was determined by ITLC-SG strips using 0.9% NaCl aqueous solution (saline) as developing solvent and simultaneously in acetone and PAW (Pyridine, acetic acid and water in 3:5:1.5 ratio). Each ITLC was cut into 0.1-cm segments, and counts of each segment were taken.

In vitro serum stability assay

The fresh human serum was prepared by allowing blood collected from healthy volunteers to clot for 1 h at 37 °C in a humidified incubator maintained at 5% carbon dioxide, 95% air. Then the sample was centrifuged at 400 rpm, and the serum was filtered through 0.22 μm syringe filter into sterile plastic culture tubes. The above freshly prepared technetium radio complexes were incubated in fresh human serum at physiological conditions, that is, at 37 °C at a concentration of 100 nM/mL and then analyzed by ITLC-SG at different time intervals to detect any dissociation of complex. Percentage of free pertechnetate at a particular time point that was estimated using saline and acetone as mobile phase, represented percentage dissociation of the complex at that particular time point in serum.

Blood kinetic studies

The blood clearance study was performed in normal rabbit, weighing 2–2.5 kg. Of the $^{99\text{m}}\text{Tc}$ -labeled compounds (0.3 mL), 5 MBq was administered intravenously through the dorsal ear vein. At different time intervals about 0.5-mL blood samples were withdrawn from the dorsal vein of other ear, and radioactivity was measured in the gamma counter. The data from the experiment were expressed as percentage of administered dose at each time interval.

Biodistribution study in mice

Albino mice strain (A) (taken in triplicate set) was used for the tissue distribution studies. Animal handling and experimentation were carried out as per the guidelines of the Institutional Animal Ethics Committee.

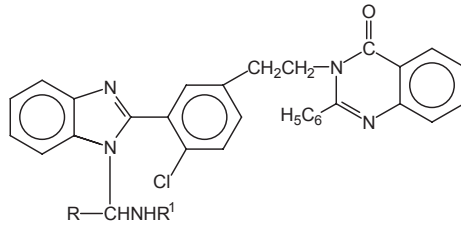
An equal dose of 10 μCi of labeled test compound was injected in mice through tail vein of each animal. At different time intervals, mice were killed, blood sample was collected, and different tissue and organs were dissected and analyzed. The radioactivity was measured in a gamma counter. The actual amount of radioactivity administered to each animal was calculated by subtracting the activity left in the tail from the activity injected. Radioactivity accumulated in each organ was expressed as percentage administered dose per gram of tissue. Total volume of the blood was calculated as 7% of the body weight.

Measurement of potential cytotoxicity

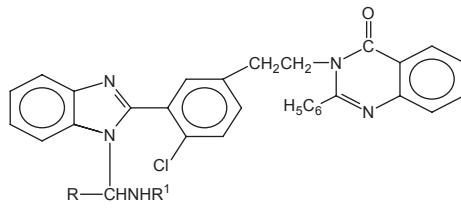
The synthesized compounds were tested against (MCF-7) human breast adenocarcinoma cell line (originally obtained in 1977, from the Michigan Cancer Foundation). Routine culture maintenance and experimental studies were carried out at 37 °C in a cell incubator with humid atmosphere at 5% CO_2 . Cell propagation was achieved in DMEM (Dubecco's modified eagle minimal medium) with phenol red, 10% fetal bovine serum, L-glutamine, penicillin, streptomycin, and gentamycin as described in the previous literature. Before any experiment, the cells were transferred for 4 days to a defined medium, containing phenol red-free DMEM, supplemented with 10% charcoal stripped. Estrogen (17 β -estradiol) in the concentration up to 100 μg was added to defined medium. Doxorubicin is taken as standard. The MTT assay with 3-(4, 5-dimethylthiazole-2-yl)-2, 5-phenyltetrazolium bromide was used to determine the number of viable cells. For assay, MCF-7 cells (1×10^4 cells/well) were plated in a 96-well tissue culture plate and exposed to the compounds under investigation. Cells were processed with the MTT assay for 24, 48, and 72 h of incubation. In brief, 10 μL of MTT (final concentration = 250 $\mu\text{g}/\text{mL}$) in PBS (phosphate buffer saline) was added to every well containing 100- μL cell suspension in medium, and the cultures were incubated at 37 °C for 5 h. The reaction mixture was carefully taken out, and 100 μL of DMSO was added to each well and pipetted up and down several times unless it became homogenic. After 10 min, the color was read at 540 nm using spectrophotometer plate reader (Bio-Rad, Tokyo, Japan). The inhibitory effect on cell proliferation was determined after 72 h of treatment with various concentrations (0.1–300 nM) of the tested compound.

Result and Discussion

In the search for useful $^{99\text{m}}\text{Tc}$ probes for early detection and staging of EGFR positive tumors, we have designed and synthesized the new ligands by modifying a known tyrosine kinase inhibitor, Skelton of quinazoline. In the scheme, the synthesis of final benzimidazole [4A–4E] was described. The structures of all the newly synthesized compounds were elucidated with different spectroscopic techniques such as IR, NMR, mass spectroscopy, and by elemental analysis

Table 1: Chemical profile of quinazoline-benzimidazole analogs **4[A]–4[E]**


Compound no.	R	R ¹	m.p. (°C)	Yield	Colour	Molecular formula	Molecular weight	Analysis	
								Calcd.	Found
1	Phenyl	4-methyl-phenyl	175–180	60	Yellow	C ₄₃ H ₃₄ N ₅ OCl	671.5	10.42	10.30
2	Phenyl	4-methoxy-phenyl	170	50	White	C ₄₃ H ₃₄ N ₅ O ₂ Cl	687.5	10.18	9.90
3	Styryl	4-methyl-phenyl	184	49	Light brown	C ₄₅ H ₃₆ N ₅ OCl	697.5	10.03	9.95
4	Styryl	7-methoxy-phenyl	162–164	51	Brown	C ₄₅ H ₃₆ N ₅ O ₂ Cl	713.5	9.81	9.50
5	4-methoxy-phenyl	4-methyl-phenyl	180–182	55	White	C ₄₄ H ₃₆ N ₅ O ₂ Cl	701.5	9.98	9.42

Table 2: Spectral analysis of quinazoline-benzimidazole analogs **4[A]–4[E]**


Compound No.	R	R ¹	Spectral analysis	LC-MS (<i>m/z</i>)
1	Phenyl	4-methyl-phenyl	IR (kBr) (ν_{\max} in cm^{-1}): 1695 (test amide C=O), 1735 (ester C=O), 1630 (C=N), 3345 (N-17). ¹ HNMR (CDCl ₃) (δ ppm): 6.75–7.60 (m, 26H, ArH), 3.25 (s, 3H, CH ₃), 3.75 (t, 2H, N-CH ₂), 2.80 (s, 1H, N-CH).	671
2	Phenyl	4-methoxy-phenyl	IR (kBr) (ν_{\max} in cm^{-1}): 1690 (test amide C=O), 1705 (ester C=O), 1630 (C=N), 3360 (N-17). ¹ HNMR (CDCl ₃) (δ ppm): 6.75–7.85 (m, 26H, ArH), 2.55 (s, 3H, OCH ₃), 3.75 (t, 2H, N-CH ₂), 2.80 (s, 1H, N-CH).	687
3	Styryl	4-methyl-phenyl	IR (kBr) (ν_{\max} in cm^{-1}): 1695 (test amide C=O), 1788 (ester C=O), 1632 (C=N), 3345 (N-17), 1130 (C=C). ¹ HNMR (CDCl ₃) (δ ppm): 6.75–7.65 (m, 26H, ArH), 3.25 (s, 3H, CH ₃), 3.85 (t, 2H, N-CH ₂), 2.80 (s, 1H, N-CH).	697
4	Styryl	7-methoxy-phenyl	IR (kBr) (ν_{\max} in cm^{-1}): 1680 (test amide C=O), 1735 (ester C=O), 1638 (C=N), 3345 (N-17), 1130 (C=C). ¹ HNMR (CDCl ₃) (δ ppm): 6.55–7.65 (m, 26H, ArH), 2.55 (s, 3H, OCH ₃), 3.72 (t, 2H, N-CH ₂), 2.80 (s, 1H, N-CH).	713
5	4-methoxy-phenyl	4-methyl-phenyl	IR (kBr) (ν_{\max} in cm^{-1}): 1690 (test amide C=O), 1735 (ester C=O), 1635 (C=N), 3340 (N-17). ¹ HNMR (CDCl ₃) (δ ppm): 6.35–7.60 (m, 26H, ArH), 3.25 (s, 3H, CH ₃), 3.70 (t, 2H, N-CH ₂), 2.80 (s, 1H, N-CH), 2.50 (s, 3H, OCH ₃).	701

(Tables 1 and 2). Comparing the TLC with the starting materials, which resulted a single spot different from the starting materials, checked the synthesized ligand. The spectral evidence confirms the presence of different functionalities (IR at 3351, 1640, 1467 cm^{-1}). Similarly, NMR multiplet in the range of (6.2–8) ppm of 5–15 hydrogen also confirms the presence of aromatic rings. It also confirms the proposed stoichiometry and structure for the phenothiazinyl

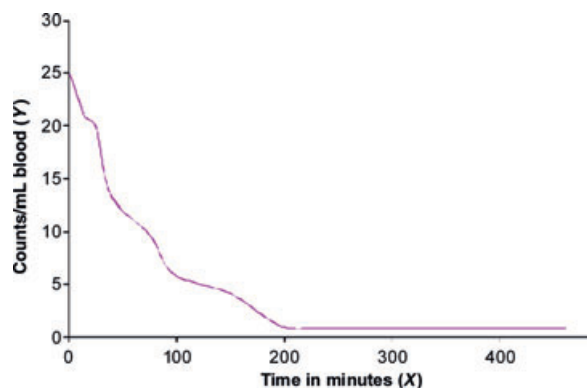
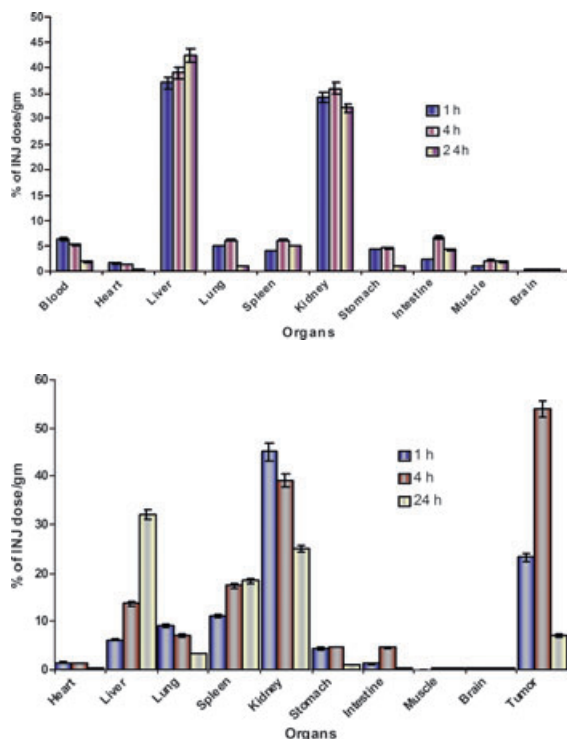
quinazolones. Integral of NMR confirms the number of protons in phenothiazinyl quinazolones as well as coupling constant confirms the nature of double bonds.

The cell proliferation was measured by MTT assay, and the results were expressed as IC₅₀ values. The activity data are given in Table 3. The inhibition of the EGFR activity by **4[A]–4[E]** was evalu-

Table 3: Antiproliferative activity of the compounds **4**[A]–**4**[E] against the MCF-7 cells and their corresponding EGFR-TK activity

Compound	IC ₅₀ (μM) EGFR-TK	IC ₅₀ (μM) MCF-7
4 [A]	0.072 ± 0.003	9.02 ± 1.24
4 [B]	0.062 ± 0.005	6.31 ± 0.41
4 [C]	0.049 ± 0.005	5.40 ± 1.34
4 [D]	0.081 ± 0.006	10.30 ± 0.39
4 [E]	0.190 ± 0.005	15.42 ± 1.52

The values are the mean ± SD of independent experiments.
Concentration of compound resulting in 50% inhibition of EGFR-TK activity.

**Figure 1:** Blood kinetic study of labeled benzimidazole analogue in rabbit **4**[C].**Figure 2:** Biodistribution study of labeled benzimidazole analogue in normal and tumor bearing mice **4**[C].

ated in human breast cancer cell line, MCF-7. These cells are also known to over-express EGFR, which leads to continuous activation of the EGFR pathway involved in cell proliferation. The inhibitory effects on MCF-7 cell proliferation were determined after 72 h of treatment with various concentrations (10^{-5} to 10^{-10} M) of the tested compound, and the results were expressed as IC₅₀ values ranging from 0.030 to 0.190 μM.

Preliminary complexation of novel synthesized compounds with ^{99m}Tc was found to give sufficiently stable complexes under physiological conditions. The *in vitro* serum stability of the radio complexes is necessary parameter meant to measure the effectiveness of chelating moiety to coordinate the radio metal. Generally, there is transchelation of radio metal to serum proteins particularly albumin. *In vitro* serum stability of the complexes clearly indicates that initially there was fall in the stability of the complex but further showing a constant stability. Initial fall in the labeling efficiency after the addition of fresh serum could be attributed to the transchelation that could have taken place in serum because of high affinity of plasma proteins for metal ions.

The retention of drug in the blood of the animal depends upon the pharmacological and physical properties of the drugs. Nearly all the phenothiazinyl quinazolones shows a very rapid clearance of radio-activity from the blood. Approximately 50–65% of activity was removed within 1 h and more than 90% in 3 h (Figure 1). It shows rapid kinetics, which may be attributed to the hydrophilic nature of the drug–radio-metal complexes.

Biodistribution of the radio complexes is an important phenomenon to study because it gives an idea about its excretory metabolic pathway and *in vivo* distribution of the radio complex drug. Accumulation of low amount of radioactivity in the stomach precludes the presence of free pertechnetate, which indicates *in vivo* stability of preparation. The percentage distribution of drug in various organs of mice is shown as percentage of injected dose per organ or tissue at different time intervals (Figure 2). The drug localized in the liver and kidneys; with the passage of time, the activity in kidney amplified for most of the compounds. This shows that the major route of excretion of activity is through kidneys. Accumulation of drugs in liver may also be because of protein binding nature of drugs. Very slight accumulation of activity was observed in lungs, spleen, and stomach. Negligible accumulation occurs in heart and brain. Biodistribution in tumor-bearing mice showed that the compound is specific for tumor cells, so, further it can be used for diagnostic purpose through SPECT/scintigraphic techniques. Biodistribution of the ^{99m}Tc complex in healthy animals showed a rather fast blood and soft tissue clearance between 0 and 2 h, followed by a slower clearance between 2 and 6 h.

Conclusion

Because breast cells are known to overexpress EGFR, which leads to continuous activation of the EGFR pathway involved in cell proliferation, and therefore, we measured antitumor activity of the compounds *in vitro* on human breast carcinoma cell line (MCF-7). Most of the tested compounds exhibited potent inhibitory activity against MCF-7 cell line.

These preliminary encouraging results of biological screening of the tested compounds could offer an excellent framework in this field that may lead to the discovery of potent antitumor agent.

Conflict of Interest

This is also certified that there is no interest of conflict between authors of manuscript.

References

- Szezepankiewicz W., Wagner P., Suwinski J. (2003) Transformation of 5, 5-diaryl-4, 5-dihydro-1, 2, 4-oxadiazoles to 4-arylquinazolines. *Tetrahedron Lett*;44:2015–2017.
- Kumar V., Mohan C., Mahajan M.P. (2005) A catalyst- and solvent-free selective approach to biologically important quinazolines and benzo[*g*]quinazoline. *Tetrahedron*;61:3533.
- Dandia A., Singh R. (2005) Green chemical multi-component one-pot synthesis of fluorinated 2,3-disubstituted quinazolin-4(3*H*)-ones under solvent-free conditions and their anti-fungal activity. *J Flour Chem*;126:307–312.
- Alagarsamy V, Thangathirupathy A, Mandal SC, Rajasekaran S, Vijaykumar S. (2006) Pharmacological evaluation of 2-substituted (1, 3, 4) thiadiazolo quinazolines. *Indian J Pharm Sci*;68:108–111.
- Malecki N., Caroto P., Rigo B., Goossens J.H., Henchart J.P. (2004) Synthesis of condensed quinolines and quinazolines as DNA ligands. *Bioorg Med Chem*;12:641.
- Bertelli L., Biagi G., Giorgi I., Barili P.L. (2000) Substituted 1, 2, 3-triazolo[1,5-*a*] quinazolines: synthesis and binding to benzodiazepine and adenosine receptors. *Eur J Med Chem*;35:333.
- Tiwari A.K., Mishra A.K., Singh V.K. (2006) Synthesis and pharmacological study of novel pyrido-quinazolone analogues as anti-fungal, antibacterial, and anticancer agents. *Bioorg Med Chem Lett*;16:4581–4585.
- Ram VJ, Farhanullah M, Tripathi BK, Srivastava AK (2003) Synthesis and antihyperglycemic activity of suitably functionalized 3*H*-quinzolin-4-ones. *Bioorg Med Chem*;11:2439–2444.
- Kochler R., Goodman L., Baker B.R. (1958) Potential anticancer agents. IX. Tetrahydroquinazoline analogs of tetrahydrofolic acid. I. *J Am Chem Soc*;80:5779.
- Hynes J.B., Buch J.M., Freisheim J.H. (1975) Quinazolines as inhibitors of dihydrofolate reductase. 3. Analogs of pteric and isopteroic acids. *J Med Chem*;18:1191.
- Alagarsamy V, Murugananthan G, Venkateshperumal R (2003) Synthesis, analgesic, anti-inflammatory and antibacterial activities of some novel 2-methyl-3-substituted quinazolin-4(3*H*)-ones. *Biol Pharm Bull*;26:1711.
- Volzhina ON, Yakhontov LN (1982) Quinazoline cardiovascular agents. *Pharm Chem J*;16:734–741.
- Campbell S.F., Davey M.J., Hartstone J.D., Lewis B.N., Palmer M.J. (1987) 2, 4-diamino-6, 7-dimethoxyquinazolines. 1. 2-[4-(1, 4-Benzodioxan-2-ylcarbonyl)piperazin-1-yl] derivatives as alpha 1-adrenoceptor antagonists and antihypertensive agents. *J Med Chem*;30:49–57.
- Charpiot B, Brun J, Donze I, Naef R, Stefani M, Mueller T. (1998) Quinazolines: combined type 3 and 4 phosphodiesterase inhibitors. *Bioorg Med Chem Lett*;8:2891–2896.
- Fukunaga J.Y., Hansch C., Steller E.E. (1976) Inhibition of dihydrofolate reductase. Structure-activity correlations of quinazolines. *J Med Chem*;19:605–611.
- Elslager E.F., Johnson J.L., Werbel L.M. (1983) Folate antagonists. 20. Synthesis and antitumor and antimalarial properties of trimetrexate and related 6-[(phenylamino) methyl]-2, 4-quinazolin-4-aminos. *J Med Chem*;26:1753–1760.
- Kung P.P., Casper M.D., Cook K.L., Wilson-Lingardo L. (1999) Structure-activity relationships of novel 2-substituted quinazoline antibacterial agents. *J Med Chem*;42:4705–4713.
- Saeki T., Adachi Y. (1995) A selective type V phosphodiesterase inhibitor, E4021, dilates porcine large coronary artery. *J Pharmacol Exp Ther*;272:825–831.
- Ogawa N., Yoshida T., Aratani T., Koshinaka E., Kato H., Ito Y. (1988) Synthesis and histamine H₂-antagonist activity of 4-quinazolinone derivatives. *Chem Pharm Bull*;36:2955–2967.
- Hans H.J., Cronin T.H. (1968) Antihypertensive 2-amino-4(3*H*)-quinazolinones. *J Med Chem*;11:130–136.
- Witt A., Bergman J. (2003) Recent developments in the field of quinazoline chemistry. *Curr Org Chem*;7:659–677.
- Davoll J., Johnson A.M. (1970) Quinazoline analogues of folic acid. *J Chem Soc C*;8:997–1002.
- Mendelsohn J., Baselga J. (2000) The EGF receptor family as targets for cancer therapy. *Oncogene*;19:6550–6565.
- Cruickshank R., Duguid J.P., Marion B.P., Swain R.H.A. (1975) *Medicinal Microbiology*, 12th edn, Vol. 2. London: Churchill Livingstone;pp. 196–202.
- Collins A.H. (1976) *Microbiological Methods*, 2nd edn. London: Butterworth.
- Khan Z.K. (1997) In vitro and vivo screening techniques for bioactivity screening and evaluation. *Proceeding Int. Workshop UNIDO-CDRI*, pp. 210–211.
- Varma R.S. (1998) *Antifungal Agents: Past, Present and Future Prospects*. Lucknow, India: National Academy of Chemistry and Biology.
- Chhikara B.S., Kumar N., Tandon V., Mishra A.K. (2005) Synthesis and evaluation of bifunctional chelating agents derived from bis(2-aminophenylthio) alkane for radio imaging with ^{99m}Tc. *Bioorg Med Chem*;13:4713–4720.
- Kumari S., Kalra N., Mishra P., Chutani K., Mishra A., Chopra M. (2004) Novel ^{99m}Tc radiolabeled quinazolinones derivative [Qn-In]: synthesis, evaluation and biodistribution studies in mice and rabbit. *Nucl Med Biol*;31:1087–1095.